Proc. of the 9th International Symposium on Geotechnical Safety and Risk (ISGSR)
Edited by Zhongqiang Liu, Jian Dai and Kate Robinson
Published by Research Publishing, Singapore. ©2025 The Author(s), CC-BY 4.0 licence.
doi: 10.3850/GRF-25280825_isgsr-144-P358-cd

PHYSICAL-INFORMED NEURAL NETWORK FOR PREDICTING SPATIOTEMPORAL VARIATION OF PORE WATER PRESSURE IN SOILS DUE TO CONSOLIDATION

Shuairong Wang[1], Shuai Zhang[1], Jiang Qian[2]

[1] *MOE Key Laboratory of Soft Soils and Geo-Environmental Engineering, Zhejiang University, Hangzhou, Zhejiang, China.*
E-mail: wangshuairong@zju.edu.cn; zhangshuaiqj@zju.edu.cn
[2]*Sun Hung Kai Properties Limited, Hong Kong, China.*
E-mail: jcqian@shkp.com.cn

Rapid urbanization has caused numerous construction solid waste landfills. The historical stepwise landfilling process may generate excess porewater pressure (PWP) within the slope, dissipatinggradually due to the consolidation. Accurately modeling the spatiotemporal variation of PWP is essential for keeping slope stability. The physical-informed neural networks (PINNs) provide a promising approach for predicting soil responses in geoengineering. However, PINNs' training is often unstable and inefficient. This study develops a novel PINN framework with an enhanced network architecture to model soil consolidation behaviors. The enhanced architecture modifies the traditional fully connected neural networks (FNNs) by adding two additional transformer networks. Compared to the vanilla PINNs with traditional FNNs, the novel PINNs demonstrate enhanced training stability inforward simulation and convergence speed in the inverse analysis through a benchmark test of Terzaghi's problem. The novel PINNs are then used to model a consolidation problem close to real-world scenarios with continuous drainage boundary conditions and noisy monitoring data. The results demonstrate that the novel PINNs can accurately identify the coefficient of consolidation and interface parameters simultaneously in a noise dataset. Furthermore, the model not only reconstructs the excess PWP variation at the sampled locations but also provides reliable prediction in the unsampled areas, demonstrating the physical interpretability of PINNs. This methodology offers a new idea for developing a geo-digital twin model by incorporating real monitoring data and respecting the physical laws.

Keywords: Data-driven; Physical-informed; PINNs; Consolidation; Digital twin.

1. Introduction

Rapid urbanization in China has led to the proliferation of construction solid waste landfills, which pose significant safety risks to surrounding areas. During landfill construction, the porewater pressure within the landfill increases as waste soils are gradually deposited on the surface. In cases of inefficient drainage and rapid waste accumulation, the porewater pressure can build up without sufficient time for dissipation. This hinders proper consolidation of the soil and increases the potential for safety hazards. A notable example of this occurred in Shenzhen, China, where a landslide destroyed 33 buildings and 77 fatalities (Wang et al., 2024; Zhang et al., 2024). To prevent similar disasters, it is crucial to study the response of pore water pressure under surface loading conditions.

The physics-informed neural network (PINN) presents a novel framework for solving problems governed by partial differential equations (PDEs) and integrating sensor data (Raissi et al., 2019). This approach leverages neural networks to approximate unknown solutions while adhering to physical laws and observed data. PINNs can serve as pure PDE solvers for forward simulations or as tools for inverse analysis, estimating unknown parameters by integrating observed information. This versatility has enabled their application across multiple fields (Karniadakis et al., 2021).

However, PINN training often exhibits large oscillations and inefficiency. This study aims to develop a novel PINN framework with an enhanced network architecture to model the consolidation problem with high efficiency and training stability. It will conduct both forward simulations to predict excess PWP responses under surface loading and inverse analyses to estimate unknown soil parameters based on monitoring data.

2. Theory of Terzaghi's consolidation problem

2.1. *Governing equations*

The governing equation of the one-dimensional Terzaghi's consolidation theory is expressed as follows (Bekele, 2021):

$$\frac{\partial u}{\partial t} - C_v \frac{\partial^2 u}{\partial z^2} = 0 \quad (1)$$

where u is the incremental porewater pressure due to the surface loading, z and t are the spatiotemporal coordinates, and C_v is the coefficient of consolidation.

2.2. *Dimensionless form of PDEs*

Nondimensionalizing the PDEs system plays a critical role in training PINNs, which can facilitate stable forward and backward propagation and enhance convergence (Wang et al., 2023). This study introduces a suitable dimensionless form of the PDE of the classical Terzaghi's consolidation theory. Let $\bar{\circ}$ be the dimensionless variables, i.e.,

$$\bar{z}_i = \frac{z_i}{\dot{z}},\ \bar{t} = \frac{t}{\dot{t}},\ \bar{u}_i = \frac{u_i}{\dot{u}}, \dot{t} = \frac{\dot{z}^2}{C_v} \quad (2)$$

where $\dot{z}$ denotes the length of the soil column (m), $\dot{u}$ denotes the surface loading (N/m^2), and $\dot{t}$ is the temporal dimensionless factor. Then the dimensionless form of Eq. (1) can be expressed as:

$$\frac{\partial \bar{u}}{\partial \bar{t}} - \frac{\partial^2 \bar{u}}{\partial \bar{z}^2} = 0 \quad (3)$$

Given the inverse analysis of the unknown coefficient of consolidation, its corresponding term should not be omitted, i.e.,

$$\frac{\partial \bar{u}}{\partial \bar{t}} - \frac{C_v}{C_v^0}\frac{\partial^2 \bar{u}}{\partial \bar{z}^2} = 0 \quad (4)$$

where C_v^0 can be regarded as a prior value derived from empirical knowledge.

3. PINNs for Terzaghi's problem

3.1. Vanilla PINNs

The vanilla PINNs aim to approximate the solution variables of physical phenomena using fully connected neural networks (FNNs) (Raissi et al., 2019). Within the PINNs framework, the neural network parameters are trained to minimize a composite loss function $\mathcal{L}(z, t; \boldsymbol{\theta})$. It can be expressed as follows:

$$\mathcal{L}(z,t;\boldsymbol{\theta}) = \mathcal{L}_f(z_f,t_f;\boldsymbol{\theta}) + \mathcal{L}_i(z_i,t_i;\boldsymbol{\theta}) + \mathcal{L}_b(z_b,t_b;\boldsymbol{\theta}) + \mathcal{L}_s(z_s,t_s;\boldsymbol{\theta}) \quad (5)$$

where $\mathcal{L}_f(z_f, t_f; \boldsymbol{\theta})$ is the loss term of governing equations, $\mathcal{L}_i(z_i, t_i; \boldsymbol{\theta})$ and $\mathcal{L}_b(z_b, t_b; \boldsymbol{\theta})$ are the loss terms from initial and boundary conditions, respectively, $\mathcal{L}_s(z_s, t_s; \boldsymbol{\theta})$ is the loss term of monitoring data, and $\boldsymbol{\theta}$ denotes the trainable network parameters, i.e., weights and biases. Given the forward simulation, the loss term of monitoring data can be omitted. In contrast, it should be retained for the inverse analysis. The procedure to calculate each loss term can be defined as mean squared errors, i.e.,

$$\mathcal{L}_f(z_f,t_f;\boldsymbol{\theta}) = \frac{1}{N_f}\sum\left|\frac{\partial \hat{\bar{u}}}{\partial \bar{t}_f} - \frac{\partial^2 \hat{\bar{u}}}{\partial \bar{z}_f^2}\right|^2 \text{ or } \mathcal{L}_f(z_f,t_f;\boldsymbol{\theta}) = \frac{1}{N_f}\sum\left|\frac{\partial \hat{\bar{u}}}{\partial \bar{t}_f} - \frac{C_v}{C_v^0}\frac{\partial^2 \hat{\bar{u}}}{\partial \bar{z}_f^2}\right|^2 \quad (6)$$

$$\mathcal{L}_i(\bar{z}_i,\bar{t}_i;\boldsymbol{\theta}) = \frac{1}{N_i}\sum\left|\hat{\bar{u}} - \tilde{\bar{u}}\right|^2 \quad (7)$$

$$\mathcal{L}_b(\bar{z}_b,\bar{t}_b;\boldsymbol{\theta}) = \frac{1}{N_b}\sum\left[\left|\hat{\bar{u}} - \tilde{\bar{u}}\right|^2 + \left|\frac{\partial \hat{\bar{u}}}{\partial \bar{z}} - \frac{\partial \tilde{\bar{u}}}{\partial \bar{z}}\right|^2\right] \quad (8)$$

$$\mathcal{L}_s(\bar{z}_s,\bar{t}_s;\boldsymbol{\theta}) = \frac{1}{N_s}\sum\left|\hat{\bar{u}} - \tilde{\bar{u}}\right|^2 \quad (9)$$

where $\hat{\bullet}$ indicates the predicted solutions by neural networks and $\tilde{\bullet}$ indicates the real solutions, N_f, N_i, N_b, and N_s are the collocation points for each corresponding loss term. The derivative of each input variable in the loss

calculation can be efficiently determined using Automatic Differentiation. By minimizing the total loss, the optimal network parameters are progressively learned.

3.2. Enhanced PINNs with modified FNNs

This study adopts an innovative architecture of modified fully connected neural networks (FNNs) proposed by Wang et al. (2021) to develop an enhanced PINNs. Compared to conventional FNN architectures, the modified FNNs demonstrate superior training stability and efficiency in this study. Drawing inspiration from neural attention mechanisms in computer vision, this architecture introduces two additional transformer networks that perform two critical functions: (1) mapping input variables into a high-dimensional feature space and (2) adjusting the forward propagation process within the hidden layers. The detailed propagation procedure of this architecture can refer to Wang et al. (2021).

4. Benchmark experiments

The one-dimensional Terzaghi's problem is first employed to illustrate forward simulations and inverse analysis performances of the enhanced PINNs compared to vanilla PINNs. Terzaghi's problem considers a sandy soil column with a length of L = 10 m (Fig. 1). The coefficient of consolidation is assumed to be 0.09 m^2/s. A surface load of P_0 = 100 kPa is applied, and the temporal domain for this analysis is limited to 2000 s. The upper boundary is maintained at zero porewater pressure, while the lower boundary is impermeable. The corresponding analytical solution is listed in the appendix.

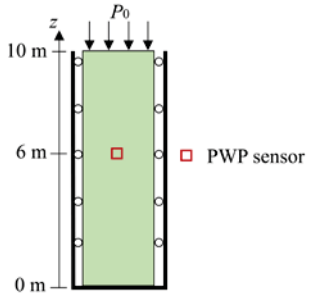

Fig. 1. Sketch of the one-dimensional Terzaghi's problem.

In the PINNs training, 4000 collocation points are used to optimize PDE residuals, with 500 and 80 points for initial and boundary conditions, respectively. These points are randomly sampled at each epoch. The traditional FNNs employ 3 hidden layers and 64 neurons in each layer. The modified FNNs retain the same configuration for the hidden layers as the traditional FNNs but incorporate two additional transformer networks, each with 1 hidden layer and 64 neurons. All networks are initialized using the Xavier scheme. The training process for both approaches employs 50,000 epochs. The Tanh is the activation function and the Adam is the optimizer, with a learning rate of 10^{-3}. All algorithms are implemented by PyTorch.

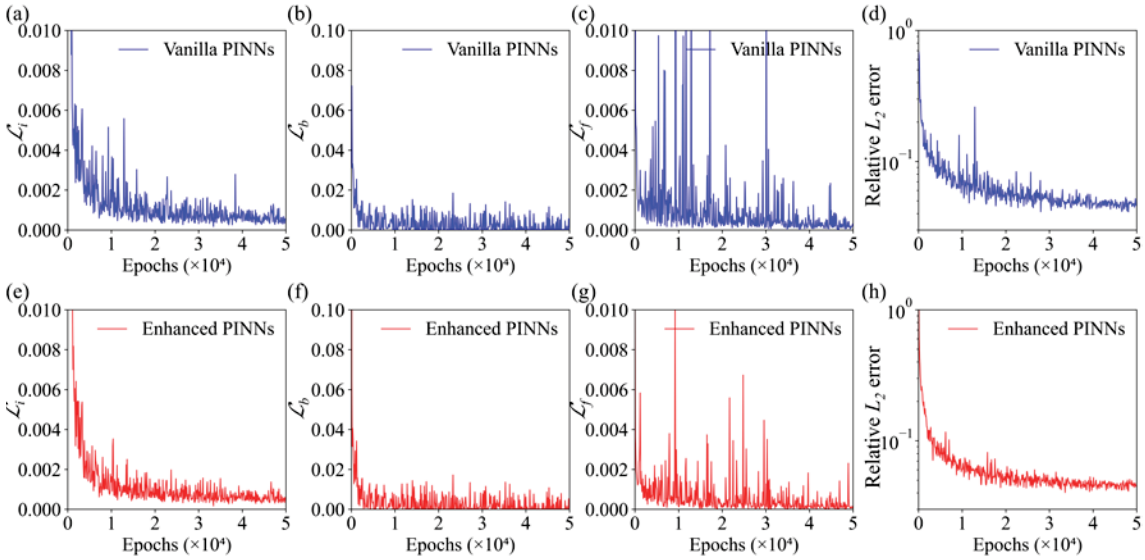

Fig. 2. The evolutions of three loss terms of initial condition($\mathcal{L}_i$), boundary condition ($\mathcal{L}_b$), and governing equations ($\mathcal{L}_f$), and the relative L_2 error of excess PWP predictions by both models.

4.1. *Forward simulation*

Figure 2 displays the evolutions of three loss termsof initial condition($\mathcal{L}_i$), boundary condition ($\mathcal{L}_b$), and governing equations ($\mathcal{L}_f$), and the relative L_2 error of excess PWP predictions by both models. Relative L_2 error represents the predictive performance of the PINNs model. All loss terms are gradually converging to steady states. Comparative analysis reveals that the enhanced PINNs exhibit reduced oscillation patterns in the relative L_2 error evolutions. This stability enhancement in the training process illustrates the superior performance of the modified FNNs over traditional FNNs. Figure 3 illustrates the analytical solutions and predictions by the enhanced PINNs for the excess PWP. The predictions by the enhanced PINNs closely align with the analytical solution, demonstrating outstanding performance in forward simulation.

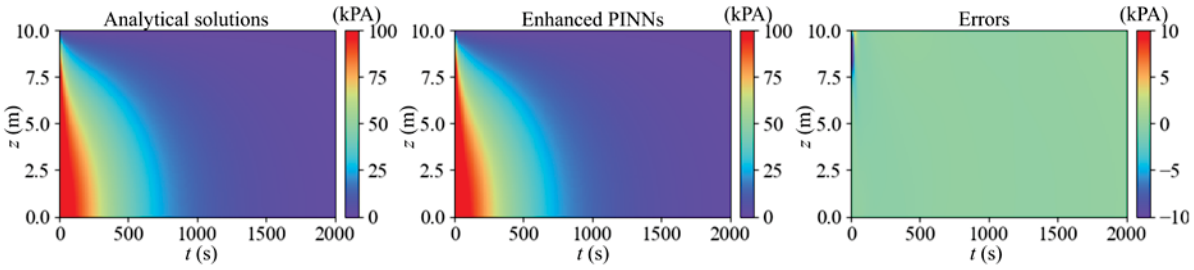

Fig. 3. Analytical and predicted solutions by the enhanced PINNs for the variation of the excess PWP.

4.2. *Inverse analysis*

The monitoring system utilizes a PWP sensor installed at a height of 6 meters (Fig. 1). The PINN training process integrates both the loss terms derived from the physical law of PDEs and the monitoring data to conduct inverse analysis. Figure 4 illustrates the evolution of the inverse-calculated coefficients of consolidation obtained through both enhanced and vanilla PINNs. In both approaches, the predicted C_v values progressively converge to the true value of 0.09 m²/s, highlighting the significant advantage of PINNs in estimating unknown parameters. Moreover, the enhanced PINNs demonstrate faster convergence of the inverse-calculated C_v to the exact value compared to the vanilla PINNs.

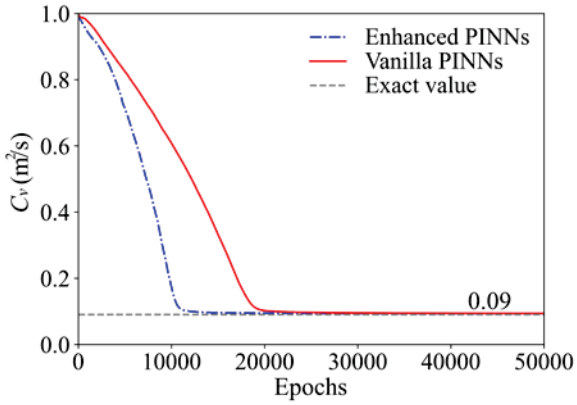

Fig. 4. The evolution of the estimated coefficient of consolidation by the enhanced and vanilla PINNs.

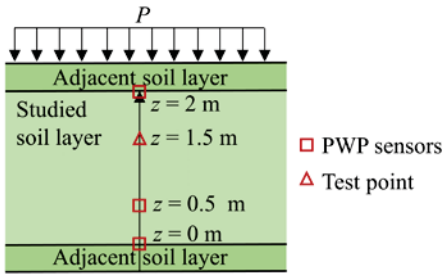

Fig. 5. Sketch of the consolidation problem with continuous drainage boundary conditions.

5. Geoengineering applications

This section further employs the enhanced PINNs to model a consolidation problem from the perspective of geoengineering applications. The PINNs are utilized to predict unknown soil parameters from noisy monitoring data. The inverse-calculated soil parameters are then used to reconstruct the variation of the target variable across the sampled and unsampled areas.

The soil profile with a thickness of 2 mis depicted in Fig. 5. Both the lower and upper boundaries are subject to continuous drainage boundary conditions, which more closely approximate real-world scenarios (Feng et al., 2019). These conditions can be mathematically expressed as follows:

$$\bar{u}(0,\bar{t}) = e^{-\alpha\bar{t}}, \quad \bar{u}(2,\bar{t}) = e^{-\beta\bar{t}} \quad (10)$$

where α and β represent the interface parameters for the lower and upper boundaries, respectively. Since the actual monitoring data is absent, the monitoring information is still derived from analytical solutions while considering additional noise interference, e.g., a 5 % noise level in this case. The analytical solutions with continuous boundary conditions can be referenced in Zhang et al. (2022). The values of ± and ² are pre-assumed to be 2 and 5, respectively. The coefficient of consolidation is set to 1.2 m²/year. Three PWP sensors are used to collect monitoring data, and their locations are shown in Fig. 5. The analysis period spans 2 years, with 20 data points sampled at each PWP sensor. A test point (Fig. 5) is established to evaluate the extrapolation performance of the enhanced PINNs in the unsampled area.

The inverse-calculated values for α, β, and C_v are 1.94, 5.03, and 1.13 m²/year, respectively. The results are close to the corresponding exact value, thereby demonstrating that the enhanced PINNs exhibit noise resistance in inverse problems and showcase their advantages in engineering applications. Figure 6 displays the noisy monitoring data and the corresponding PWP prediction at the sampled and unsampled area. The approach reconstructs the underlying trends in PWP from noise data and preserves physical consistency inunsampled regions. These findings highlight the physical interpretability of the enhanced PINNs.

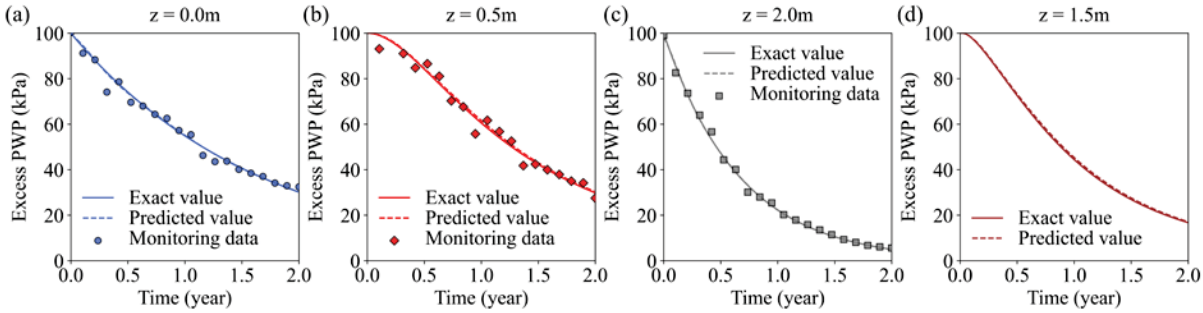

Fig. 6. The noisy monitoring data and the corresponding excess PWP predictions at the (a - c) sampled and (d) unsampled areas.

6. Conclusions

This study develops a novel PINN framework with an enhanced network architecture to model soil consolidation behaviors. The enhanced architecture modifies the traditional FNNs by adding two additional transformer networks. Through a benchmark test of Terzaghi's problem, the novel PINNs demonstrate enhanced training stability compared to the vanilla PINNs with traditional FNNs in the forward simulation. Based on the monitoring data, the inverse-calculated coefficient of consolidations by enhanced PINNs presents a faster convergence speed to the exact value than the vanilla PINNs.

To reflect the potential of the PINNs in geoengineering applications, the novel PINNs are then used to model a consolidation problem close to real-world scenarios with continuous drainage boundary conditions and noisy monitoring data. The results demonstrate that the novel PINNs can accurately identify the coefficient of consolidation and interface parameters simultaneously even in a noise dataset. Furthermore, the novel PINNs provide reliable predictions in both sampled and unsampled areas, highlighting the physical interpretability of the novel PINNs.

This study demonstrates the great advantages of the enhanced PINNs in geoengineering applications. This methodology offers a new idea for developing a geo-digital twin model by incorporating real monitoring data and respecting the physical laws. Future work should consider more complex scenarios, such as the PWP variation in real-world construction solid waste landfills, to evaluate the potential of the enhanced PINNs.

Acknowledgment
This study was funded by the National Natural Science Foundation of China (Grant No. 51988101; Grant No. 52278376).

Appendix A. The analytical solution of one-dimensional Terzaghi's problem
The analytical solutions of the incremental porewater pressure and the vertical displacement are expressed as (Biot, 1941; Castelletto et al., 2015):

$$p(z,t) = -\frac{4}{\pi} P_0 \sum_{m=0}^{\infty} \frac{(-1)^m}{2m+1} \cos\left(\frac{(2m+1)\pi z}{2L}\right) \exp\left[-\frac{(2m+1)^2 \pi^2 K_{dr}^{1D} K_{sat} t}{4L^2 \gamma_w}\right] \quad \text{(A.1)}$$

References
Bekele, Y.W., 2021. Physics-informed deep learning for one-dimensional consolidation. J. Rock Mech. Geotech. Eng. 13 (2), 420-430. https://doi.org/10.1016/j.jrmge.2020.09.005

Biot, M.A., 1941. General Theory of Three - Dimensional Consolidation. J. Appl. Phys. 12 (2), 155-164. https://doi.org/10.1063/1.1712886

Castelletto, N., White, J.A., Tchelepi, H.A., 2015. Accuracy and convergence properties of the fixed-stress iterative solution of two-way coupled poromechanics. Int. J. Numer. Anal. Methods Geomech. 39 (14), 1593-1618. https://doi.org/10.1002/nag.2400

Feng, J., Ni, P., Mei, G., 2019. One-dimensional self-weight consolidation with continuous drainage boundary conditions: Solution and application to clay-drain reclamation. Int. J. Numer. Anal. Methods Geomech. 43 (8), 1634-1652. https://doi.org/10.1002/nag.2928

Karniadakis, G.E., Kevrekidis, I.G., Lu, L., Perdikaris, P., Wang, S., Yang, L., 2021. Physics-informed machine learning. Nat. Rev. Phys. 3 (6), 422-440. https://doi.org/10.1038/s42254-021-00314-5

Raissi, M., Perdikaris, P., Karniadakis, G.E., 2019. Physics-informed neural networks: A deep learning framework for solving forward and inverse problems involving nonlinear partial differential equations. J. Comput. Phys. 378 686-707. https://doi.org/10.1016/j.jcp.2018.10.045

Wang, S.F., Sankaran, S., Wang, H., Perdikaris, P., 2023. An Expert's Guide to Training Physics-informed Neural Networks. ArXiv Preprint ArXiv: 2308.08468. https://doi.org/10.48550/arXiv.2308.08468

Wang, S.F., Teng, Y.J., Perdikaris, P., 2021. Understanding and Mitigating Gradient Flow Pathologies in Physics-Informed Neural Networks. SIAM J. Sci. Comput. 43 (5), A3055-A3081. https://doi.org/10.1137/20M1318043

Wang, S.R., Zhang, S., Chen, Y.B., Peng, D.L., Xiao, T., Zhou, Y.L., Dai, C., Zhang, L.M., 2024. Probabilistic framework for quantifying human flight failure rate to landslides. Eng. Geol. 341 107723. https://doi.org/10.1016/j.enggeo.2024.107723

Zhang, S., Lan, P., Li, H.-C., Tong, C.-X., Sheng, D., 2022. Physics-informed neural networks for consolidation of soils. Engineering Computations 39 (7), 2845-2865. https://doi.org/10.1108/EC-08-2021-0492

Zhang, S., Li, C., Peng, J., Lv, Y., Wang, S., Peng, D., Bate, B., Xue, D., Zhan, L., Ouyang, C., 2024. Physical vulnerability assessment of damaged buildings to the Shenzhen catastrophic CSW landslide. Landslides 21 (5), 1023-1039. https://doi.org/10.1007/s10346-023-02200-w